# Collaborative Multi-UAV Data Fusion for SAR Applications with Moving Targets


1st Millena Cavalcanti
*Department of Informatics*
*Pontifical Catholic University of Rio de Janeiro (PUC-Rio)*
Rio de Janeiro, Brazil
mcavalcanti@inf.puc-rio.br
*Computing Department*
*Federal Rural University of Pernambuco (UFRPE)*
Pernambuco, Brazil

2nd Bruno Olivieri
*Department of Informatics*
*Pontifical Catholic University of Rio de Janeiro (PUC-Rio)*
Rio de Janeiro, Brazil
bolivieri@inf.puc-rio.br

3rd Thiago Lamenza
*Department of Informatics*
*Pontifical Catholic University of Rio de Janeiro (PUC-Rio)*
Rio de Janeiro, Brazil
tlamenza@inf.puc-rio.br

4th Markus Endler
*Department of Informatics*
*Pontifical Catholic University of Rio de Janeiro (PUC-Rio)*
Rio de Janeiro, Brazil
endler@inf.puc-rio.br



***Abstract*—Unmanned Aerial Vehicles (UAVs) are improving considerably search and rescue (SAR) operations by providing unprecedented capabilities in dynamic and hazardous environments. This study presents an innovative, collaborative multi-UAV data fusion approach that addresses the critical challenge of locating multiple moving targets within strict time constraints. This approach improves traditional search techniques by incorporating intelligent information sharing, fusion, and coordinated path planning. The core innovation of the algorithm lies in its ability to dynamically and collaboratively predict the geographical zones with the highest probability of needed rescue operations. This enables the group of UAVs to coordinate and optimize their search strategies in real-time. This research offers valuable insights into multi-UAV collaboration through high-fidelity simulations involving more than 600 different scenarios with UAV swarms and moving ground targets. The experimental results indicate that their effectiveness significantly improves as the number of UAVs increases, following a quadratic trend until it reaches a plateau. In particular, the accuracy rate remains above 90%, regardless of the number of UAVs after reaching the plateau. This suggests that while a higher density of UAVs enhances search efficiency, larger UAV swarms yield diminishing returns. Notably, the approach shows superior efficiency in environments with clustered targets, which makes it particularly suitable for disaster response scenarios that involve more concentrated target locations.**



***Index Terms*—Autonomous Agents, Search and Rescue (SAR), Unmanned Aerial Vehicles (UAV), UAV Swarm, Path Planning**


## I. Introduction

The rapid advancement and increasing popularity of Unmanned Aerial Vehicles (UAVs) have led to a substantial increase in their deployment across various applications. This expansion is largely driven by their flexibility, mobility, and accessibility. UAVs are now used in a wide range of fields [1], [2], including smart agriculture [3], surveillance [4], wildfire management [5], disaster management [6], and search and rescue (SAR) [7], [8].

In the context of SAR operations, the prompt retrieval of survivors is paramount, particularly in the aftermath of a disaster [9]. The challenge of locating static or mobile targets in the shortest possible time is further compounded by the necessity of searching a vast area that may contain potential obstacles, thereby increasing the complexity of the challenge.

UAVs have proven highly effective in SAR operations, yielding positive results. UAVs enable the autonomous completion of tasks that were once challenging or impossible for humans to accomplish [10]. UAVs offer several advantages over other technologies and solutions, including ease of deployment, low maintenance costs, time efficiency, the ability to perform multiple tasks simultaneously, fault tolerance, high mobility, and the capability to hover in areas where deploying human rescue teams would be dangerous or restricted. This capability is especially important for situations that require quick decision-making [7], [11].

A collaborative multi-UAV system enables the comprehensive search of large areas, facilitating efficient target detection and information sharing [8]. This information includes details such as target locations, status, areas of interest, and previously covered areas, which collectively enhance the efficiency and precision of the search mission. This study proposes a novel SAR approach that utilizes information fusion in multi-UAV collaborative searches for multiple dynamic targets in uncertain and expansive scenarios with time constraints.

Using peer-to-peer communication among a dynamic swarm of UAVs, information about identified targets is exchanged, including the time and location of their detection. This data


This study was financed in part by AFOSR grant FA9550-23-1-0136.

is fused at the decision level to replan the UAV group's routes based on areas of interest identified through a Gaussian distribution probability model. Alongside the information exchange among UAVs, details about the identified targets are sent to a ground station responsible for initiating monitoring and support/search efforts related to those targets. However, these actions are beyond the scope of this article.

The main contribution of this paper can be summarized as follows

- We propose a multi-sensor fusion and multi-UAV approach for the search of multiple unknown targets in dynamic environments;
- We propose and implement an algorithm for collaboratively planning and adapting UAV paths to navigate routes that maximize the probability of locating targets, considering predictable target movements.

The remainder of this paper is organized as follows: Section II presents a review of contemporary techniques and systems. Section III discusses the system model and its constraints. We detail our collaborative multi-UAV search approach in Section IV. Section V explains the experimental setup, while Section VI discusses the results obtained from these experiments. Finally, Section VII summarizes the key conclusions and outlines potential directions for future research.

## II. Related Work

Utilizing UAVs has proven to be an effective solution for addressing challenges associated with search and information gathering in environments characterized by limited accessibility or expansive search areas [2], [12]. The primary challenges and solutions pertain to risk scenarios, including SAR, disaster management, wildfire management, and target positioning [5], [6], [13]. These scenarios present similar challenges, including the necessity of conducting a comprehensive search of an expansive area, navigating a dynamic environment, and devising a path planning strategy that accounts for the environmental constraints and the targets' location as soon as possible.

Various solutions address different aspects of UAV-based SAR, considering objectives like convergence speed, area coverage, and target detection [14]. Research has focused on locating both fixed [8], [15]–[18] and mobile targets [19]–[21].

For static targets in unknown environments, Wu et al. [17] propose a Q-Learning algorithm that optimizes UAV trajectories in two phases: a rapid search phase and an optimal path-planning phase. This approach, which penalizes obstacles as negative rewards, improves convergence speed and path efficiency over DDPG [22] and IDWA [23]. Kyriakakis et al. [15] introduce the Cumulative Unmanned Aerial Vehicle Routing Problem (CUAVRP), which uses grid-based decomposition and Parallel GRASP-VND algorithms to optimize area coverage for static targets, maximizing detection success.

Yanmaz et al. [8] propose three multi-UAV path-planning algorithms—DPPP, EDDPP, and DAPP—focused on detecting and monitoring static targets while maintaining connectivity. Less adaptive approaches (DPPP and EDPPP) perform best in target coverage and convergence speed.

For dynamic targets, Alanezi et al. [19] use a motion-encoded genetic algorithm (MEGA-MP) to identify high-probability search areas. Wu et al. [20] apply a swarm-based imitative learning optimization (SBILO) algorithm, integrating BSO and TLBO, with two phases: waypoint determination and target locking by a follower drone.

## III. System Model and Constraints

This work introduces the MUDE approach, which stands for **M**ultiple **U**AVs in a **D**ynamic search **E**nvironment, aimed at identifying mobile targets with predictable movement on the ground through the use of a collaborative UAV swarm. MUDE is designed to analyze a specified area, incorporating four main components described in Figure 1. These components include: (i) *ground station*, which transmits configuration information to the UAVs, receives and stores data collected by the UAVs and functions as the launch site for the UAVs; (ii) $n$ *search UAVs* ($u_i$), which collect sensor data while flying above, making decisions in (iii) *groups* ($g_l$) composed by UAVs within communication; and searching for a previously unknown (iv) $k$ *target objects* ($o_j$) that are searched in the mission.

A mission is initiated with the following parameters:

- $A$: geographic search area;
- $T$: maximum mission duration time;
- $U = \{u_1, .., u_i, ..., u_n\}$: set of UAVs with size $n$;
- $r_c$: radius of the inter-UAV RF communication range;
- $W_i$: set of waypoints for each $u_i \in U$ (eq. 1), defining an initial route for each $u_i$;

$$W_i = [(la_{i_0}, lo_{i_0}, alt_{i_0}), ..., (la_{i_f}, lo_{i_f}, alt_{i_f})] \quad (1)$$

- $h$: expected UAV flight altitude for each waypoint.

The mission search area ($A$) is defined by four geolocation positions, represented as $A_i(latitude, longitude)$, the vertices of a square area. If area $A$ is not a square, the division into sub-areas and the UAV routes can be easily adjusted. However, for testing and explanation, we assume $A$ to be square in this article. The area $A$ is defined as a grid of identical, non-overlapping cells of area $S_{ground}$ (see equation 2). $S_{ground}$ denotes the area the UAV's detection sensor covers, as illustrated in Figure 2. We assume that the sensor is located at the center of the UAV and that the covered area is centrosymmetric to the drone projection on the ground [24], [25], resulting in a square area. The extent of the sensor coverage area varies following the designated flight altitude of the UAV, as specified in the mission parameters. For the purposes of this study, we assume that all UAVs in the mission operate at the same altitude, referred to as $h$.

$$S_{ground} = 4h^2(\sigma^2 - 1) \quad (2)$$

Each $u_i$ receives a predefined route generated for the specific mission parameters ($A$ and $n$) and the coverage path planning method selected for the mission. The generated route is defined by a group of waypoints $W_i$ for each $u_i$, with the initial and final waypoint set to the location of the ground

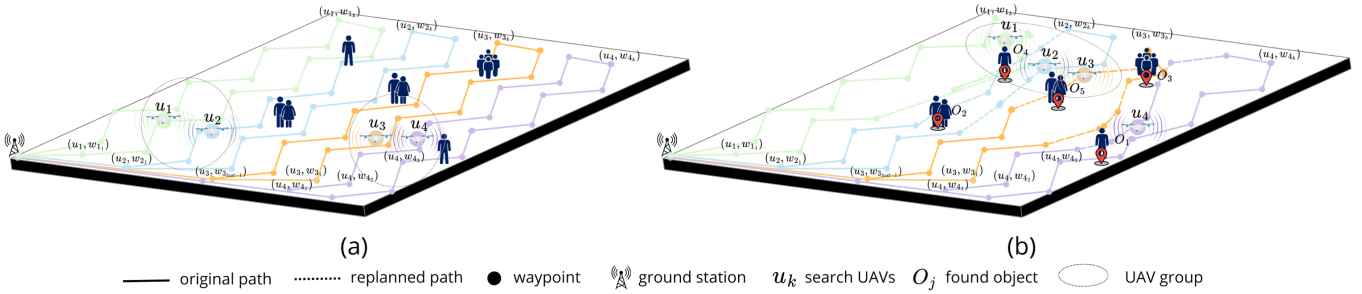


Figure 1. MUDE approach overview.

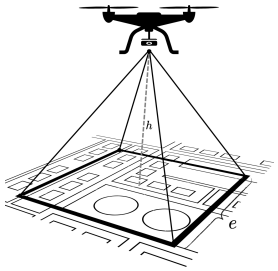


Figure 2. UAV sensor coverage of the ground area.

station. During the mission, $W_i$ is updated in each re-planned individual and social path, and some future waypoints are inserted, removed, or replaced, except for the last one, which defines the final destination of the UAV.

During the mission, each UAV $u_i$ maintains a continuously updated probability distribution grid, referred to as $M_i$. This grid is used to locate or receive target information from other UAVs. The grid $M_i$ covers the search area and comprises a mesh of points $(x, y)$ where the probability distribution is assessed. The dimensions of $M_i$ are determined by dividing the total search area $A$ by the size of the sensor's search area $S_{ground}$, resulting in a two-dimensional grid made up of $\frac{A}{S_{ground}}$ cells. Each cell's probability of finding a target at that location is modeled using a Gaussian distribution in a discretized and finite 2D space. This distribution is centered on the positions of each detected target and follows the multivariate normal distribution defined by the equation:

$$f(x,y) = \frac{1}{2\pi|\Sigma|^{1/2}} \exp\left(-\frac{1}{2}\begin{bmatrix} x-\mu_x \\ y-\mu_y \end{bmatrix}^T \Sigma^{-1} \begin{bmatrix} x-\mu_x \\ y-\mu_y \end{bmatrix}\right) \quad (3)$$

where:

- $(x, y)$ is a point in the search space;
- $\mu_x$, $\mu_y$ are the means of the distribution (target position);
- $\sum$ is the covariance matrix, which is diagonal with variance $\sigma^2 = spread^2$, and spread refers to the standard deviation of the Gaussian distribution defined as $r_c/4$.

In addition to the grid $M_i$, other parameters (listed below) related to convergence speed and the number of successful target detections are also evaluated after the mission has ended. This assessment helps to determine whether the mission was successful or not.

- $k'$: number of successful targets found.
- $TP_i$: list of target objects identified by $u_i$(eq. 4). It starts empty and records the target identification $(o_j)$, its geographical position (eq. 5), and the timestamp of its last detection.

$$TP_i = [(o_1, P_1, t_1), ..., (o_j, P_j, t_j), ..., (o_k, P_k, t_k)] \quad (4)$$

$$P_j = (la_{o_j}, lo_{o_j}) \quad (5)$$

- $t_c = t_{j_{last-object-found}}$: convergence speed;
- $C$: concentration target rate defined by eq. 6, where $l$ denotes the length of the side of the search area $A$, while $k$ represents the number of targets that have been grouped into $g$ clusters. Within these clusters, targets can be separated by a distance up to $d_{cluster}$.

$$C = \frac{g}{d_{\text{cluster}} * l^2}\left(1 - \frac{g-1}{k-1}\right) \quad (6)$$

## IV. Proposed Approach

The general goal of the MUDE approach is to provide an efficient and reliable method for detecting, identifying, and collecting information from mobile targets within a designated area using UAVs that communicate with one another. As illustrated in the pseudocode described in algorithm 1, the MUDE mission is initiated based on the parameters outlined in Section III. These parameters define various aspects of the mission, including the set of UAVs to be utilized $(U)$, the designated search area $(A)$, and the maximum duration of the mission $(T)$. Each $u_i$ starts the mission with a specific initial path, represented as a sequence of waypoints $(W_i)$, which navigates through a specified region of the search area, as directed by the ground station. The ground station generates $W_i$ based on a Coverage Path Planning (CPP) scan method, the coverage area $(A)$, and the number of UAVs $(n)$ used in the mission. $W_i$ is used to ensure the maximum area coverage of $A$. The CPP method may partition $A$ into simple flight patterns, rectangular areas with no decomposition, or $n$ grids of equal size. We employed eight CPP scanning methods for this research analysis to generate initial paths: (i) back-and-forth parallel, (ii) back-and-forth creeping line,

(iii) LMAT (Linearly Modified Approach to Trajectories), (iv) sector search, (v) random, (vi) a combination of CPP scanning methods by dividing area $A$ into $n$ grids, with one UAV assigned to each grid to execute the CPP scan method, (vii) LMAT without grid constraints, and (viii) random sampling in area $A$ without grid constraints.

The mission workflow is divided into five main stages: (i) search for targets, (ii) broadcast information about the new target found, (iii) replan social and individual path, (iv) check mission finish status, and (v)finish mission. Those stages will be explained in the following subsections (IV-A to IV-E).

Figure 1(a) illustrates the initial mission setup, featuring the predefined paths, represented by points labeled ($u_i$, $w_{i_j}$). In this notation, $i$ denotes the number assigned to the search UAV, and $j$ represents the waypoint number. For example, ($u_1$, $w_{1_4}$) indicates the fourth waypoint of the UAV $u_1$. When UAVs $u_i$ and $u_j$ are within the communication range - *i.e.,* when distance$((u_i, w_{ik}), (u_j, w_{jk})) \leq r_c$ - they form a group ($g_m$) that exchanges information about the targets discovered and collaboratively decides on a social path through consensus.

All UAVs adhere to their initial paths until they detect a target. When a UAV $u_i$ detects a target $o_k$, it verifies whether $o_k$ has already been identified. If the target is detected for the first time, $u_i$ adjusts its path to approach the area where it was located and transmits its coordinates to all other UAVs $u_k$ in the same group. This is represented in Figure 1.(a), when $u_4$ detects $o_1$ and sends its location to $u_3$, which is in the same group as $u_4$. Identifying a new target triggers a procedure to establish both the social path and the individual paths of the other UAVs. This process considers regions with the highest likelihood of finding additional targets, as defined by each UAV. The information is then fused to determine the best search areas while eliminating overlapping waypoints. Overlapping waypoints are defined as points with the exact coordinates (latitude and longitude) or those within the ground sensing coverage area of the UAV's detection sensor ($S_{ground}$).

Figure 1(b) illustrates the modified paths of the UAVs during the mission, depicted by dotted lines. It also highlights the consensus points used to determine the social path. In this figure, the group consisting of UAVs $u_1$, $u_2$, and $u_3$, shows that $u_1$ finds target $o_4$, while $u_3$ locates target $o_4$. After reaching a consensus, $u_1$, $u_2$, and $u_3$ all adjust their paths, as indicated by the dotted lines.

### A. Search for targets

Upon the mission initiation, $u_i$ moves toward its next waypoint with a constant velocity, designated as $v$. During its flight, $u_i$ continuously scans its sensor coverage area for potential targets. Once a target is identified, $u_i$ stores pertinent information about the target identification ($o_j$), which includes the target's geocoordinates ($P_j$) and the timestamp of discovery $t_j$. This information is saved as a tuple: ($o_j$, $P_j$($l_{a_{o_j}}$, $l_{o_{o_j}}$), $t_j$) in the found target list $TP_i$ of $u_i$. The details about the identified target are also broadcast to other UAVs within the communication range (see section IV-B). If no target is found, the UAV checks whether the mission is completed (see section IV-D) or continues to the next waypoint.

When $u_i$ enters the communication range of another UAV $u_j$ during its flight, the two UAVs exchange their lists of identified targets, $TP_i$ and $TP_j$, respectively. This communication exchange executes an early-level fusion in $u_i$ and $u_j$, resulting in a single merged list for both UAVs ($TP'_1 = TP'_j = TP_i \cup TP_j$) while excluding duplicate targets. Both UAVs then update their probability maps, $M_i$ and $M_j$, incorporating the information about the targets fused during the communication.

However, if $u_j$ is not a member of the group $g_m$ to which $u_i$ belongs, it also initiates the reorganization of $g_m$. Reorganization is carried out by sending a PING broadcast message from both $u_i$ and $u_j$, which allows each UAV to identify other UAVs within the communication range of either of them. UAVs within the communication range of $u_j$ that belong to a previous group $g_n$ are merged into the group $g_m$, forming a unified group $g_m$. The updated list of UAVs in this merged group is then distributed to all group members, with a

**Algorithm 1** Mission Execution

**Require:** $(A, T, t_s, h, n, U, r_c, scan\_type)$
**for** $\forall u_i \in U$ **do**
  $W_i \leftarrow generateWaypoints(i, n, A, scan\_type)$
  $t_{t_i} \leftarrow 0$
  $TP \leftarrow \emptyset$
  Start $u_i$ mission with $T$, $h_i$
  **while** mission is active **do**
    Execute **Search Targets** ▷ *(Sec. IV-A)*
    **if** target $o_k$ is found **then**
      **if** $o_k \in TP$ **then**
        Update $o_k$ position in TP
      **else**
        *// Change Individual Path (Sec. IV-C)*
        $t_k$, $t_{last-object-found} \leftarrow$ present time
        $TP \leftarrow TP \cup \{(o_k, P_k, t_k)\}$
        $M_i \leftarrow$ **updateProbabilityMap()**
        $w_h \leftarrow getPositionHighProbability(M_i)$
        $(u_i, w_{i_j}) \leftarrow midpoint(P_j, w_h)$
        Insert $(u_i, w_{i_j})$ in $W_i[next\_position]$
        Start $TIMEOUT_{ChangeRoute}$
        Travel to waypoint $(u_i, w_{i_j})$
        *// Broadcast information*
        Create message $m_f$
        $m_f.type \leftarrow START\_CONSENSUS$
        $m_f.target \leftarrow (o_k, P_k, t_k)$
        $round \leftarrow round + 1$
        $m_f.round \leftarrow round$
        $m_f.proposer \leftarrow u_i.id$
        Send a broadcast message $m_f$ ▷ *(Sec. IV-B)*
        Execute Social Path Consensus ▷ *(Sec. IV-C)*
        Start $TIMEOUT_{SC}$
      **end if**
    **else**
      **if** current_time = T **then** ▷ *(Sec. IV-D)*
        $t_{i_c} \leftarrow t_{i_{last-object-found}}$
        Travel to ground station position
        Terminate mission ▷ *(Sec. IV-E)*
      **end if**
    **end if**
    **if** $current\_time = TIMEOUT_{ChangeRoute}$ **then**
      Stop $TIMEOUT_{ChangeRoute}$
      Travel to waypoint $W_i[next\_position]$
    **end if**
  **end while**
**end for**

fusion of information about the target finds and their location, collaborating to create more realistic probability maps. This information and the dynamic reorganization of UAV groups enable better coordination and more effective target identification, considering the time constraints characteristic of SAR missions.

### B. Broadcast information

Once the $TP$ of any $u_i \in g_m$ has been modified, the updated $TP_i$ is transmitted via broadcast to all other $u_j \in g_m$, even if $u_j$ is not within the communication range of $u_i$. This exchange of information among UAVs that are out of communication range is achieved by repeating the information to the initially received UAVs.

The information related to the newly established waypoint and the identified sensor geolocation is also broadcast to the other UAVs in the group, thereby initiating a consensus decision regarding the group's social path (Algorithm 1, lines 22-31). To this end, the UAVs implement the Fast Paxos Consensus Algorithm [26], wherein the $u_i$ assumes the roles of proposer and leader at the outset of the consensus round. The acceptors, represented by the other $u_j \in g_m$, receive the $o_m$ geolocation. If $u_i.round \geq u_j.round$, then $u_j$ updates its probability distribution grid $M_j$, calculates the position $P_{j_h}$ in $M_j$ with the greater probability of finding a target, and sends $P_{j_h}$ back to $u_i$ in response to the consensus request.

After $u_i$ receives all necessary acknowledgment (ACK) messages from acceptors ($u_j \in g_m$), as defined by the Paxos consensus algorithm, containing their $P_{j_h}$, it performs a feature-level fusion with all the received $P_{j_h}$ values. This process allows it to calculate a new high probability region of interest defined by the geolocation position $P'_{i_h}$. After determining $P'_{i_h}$, it is sent to the group, updating their $M_j$ and communicating their three to five subsequent planned waypoints.

After receiving the set of waypoints, $u_i$ merges all the potential following waypoints from all $u_j$. This fused information is used by $u_i$ to determine the potential future common location of all $u_j$. The combined data and the high-probability areas containing targets enable $u_i$ to execute its individual path replan (as detailed in section IV-C) and identify coordination that the other UAVs should avoid. Subsequently, $u_i$ transmits a decision comprising a list of common waypoints to $u_j$, thereby preventing them from proceeding to the same area when replanning their individual paths.

### C. UAV Route Change Algorithm

This work examines targets with a predefined tendency to move in unison while seeking proximity. This type of behavior is observed in various scenarios, including the movements of social animals and the tendency of groups of people to gather in risky situations [27]. Given this movement pattern, UAVs can concentrate on identifying regions where groups of targets are located instead of performing a comprehensive scan of the entire area. When a UAV detects a target or a group of targets that have not yet been identified, the subsequent waypoint of the original path is stored, and a new waypoint is calculated toward a nearby location where other mobile sensors may be present (Algorithm 1, lines 12-21).

To determine the next waypoint of its path, $u_i$ updates $M_i$, considering the newfound target(s) location(s) and applying a discretized Gaussian distribution defined in Eq. 3. With the location $P_k$ of the last target found $o_k$ and the highest probability coordination to find new targets $P_{i_h}$, $u_i$ calculates mead point of ($P_k$, $P_{i_h}$) and inserts it into its $W_i$ as the next waypoint to be reached, changing its route and initiating a timer, designated as $TIMEOUT_{route\_change}$. $u_i$ continues in the new direction until the timer $TIMEOUT_{route\_change}$ is fired. In the meantime, if a new target is identified during the $TIMEOUT_{route\_change}$ time interval, the calculation of the new waypoint is repeated, following the stages outlined in IV-A, IV-B, and IV-C. If no new target is identified, the UAV reverts to its original route, resuming its flight path from where it was last altered.

The presence of targets near waypoint $(u_4, w_{4_2})$, as illustrated in Figure 1(a), triggers a route change for $u_4$. Initially, the UAV begins its tracking mission by following a predetermined path consisting of waypoints $(u_4, w_{4_1}), (u_4, w_{4_2}), (u_4, w_{4_3}), \ldots, (u_4, w_{4_k}), \ldots$. Upon reaching the waypoint $(u_4, w_{4_2})$, a target group is identified, prompting $u_4$ to change its route. The timer $TIMEOUT_{route\_change}$ starts, and the mean geographic coordinates are calculated, resulting in a new waypoint $(u_4, w_{4_3})$ that replaces the previous one as the next stop on the new route. $u_4$ continues to calculate new coordinate waypoints until $TIMEOUT_{route\_change}$ expires and no additional targets are identified. At this point, at $(u_4, w_{4k-1})$, $u_4$ resumes its original path to the next waypoint of the initial route that has not yet been reached, $(u_4, w_{4_k})$, and follows it until it reaches the endpoint or detects another target, which would trigger another route change. As the route change for $u_4$ is broadcast to the other UAVs in the group, $u_3$'s route is also modified, as depicted in Figure 1(b).

### D. Check mission finish status

After each search stage (see section IV-A) at step $t_j$, if a target has not been identified, the criteria for terminating the mission are evaluated. Each UAV checks whether $t_j$ is equal to $T$ or if it has reached waypoint $(u_i, w_{i_{last-1}})$ (Algorithm 1, lines 34-43). The UAV will initiate the mission's conclusion if either of these conditions is met.

### E. Finish mission

In the completion phase, if the UAV has not reached the final waypoint defined in the initial set of waypoints, which may also be the same as the starting point, it will update its route by designating the final waypoint as the next waypoint and proceed directly to it. While en route, the UAV may identify additional targets, but will not alter its path again.

Once the UAV reaches its designated endpoint, it will transmit all stored logs to a ground station. These logs include a comprehensive record of all traveled paths, communication

data, and identified targets. By analyzing the collected information from all UAVs in the mission, we can consolidate details related to mission completion and success rates. This analysis identifies the number of targets found ($k'$) and checks whether $k' = k$. If $k' = k$, the mission is considered successful and achieves an accuracy rate of 100%. Once all targets are identified, we also determine the convergence speed ($t_c$) and the travel time ($t_{t_i}$) of each UAV ($u_i$). If $k' \leq k$, the mission is deemed unsuccessful, and the accuracy rate is calculated as $\alpha = k'/k$.

## V. Experiments Architecture

The proposed approach was implemented and simulated using GrADyS-SIM NextGen [28], a Python framework designed explicitly for simulating distributed algorithms in a network environment comprised of communicating and mobile nodes. GrADyS-SIM NextGen enhances the original GrADyS-SIM framework [29], [30] by allowing users to simulate the same code in both integrated modes, utilizing OMNeT++ [31] for more realistic simulations of network interactions. This framework was employed to model and observe UAV swarms' movement and message exchanges, thereby validating communication and cooperation among UAVs, ground stations, and mobile targets.

Based on the system model parameters presented in Section III, 648 scenarios were modeled to analyze the algorithm's effectiveness across various parameter configurations. Each scenario consisted of two parts: (i) the environment and (ii) the mission. The environments were modeled as square search areas ($A$) containing $k$ targets organized into $c$ clusters. The mission, as described in Section III, was defined by its initial parameters, including the area ($A$), maximum mission duration ($T$), a set of UAVs ($U$) with size $n$, the UAV transmission range ($r_c$), a set of initial waypoints ($W_i$), and the UAV flight altitude ($h$), that defines the ground search area (see eq.2) of each UAV.

The search area $A$ was a series of varying-sized discrete square polygons. An exhaustive set of different scenarios was designed to investigate how UAV density and target clustering affect the efficiency and speed of the MUDE search algorithm by exploring all possible configurations of environments and missions. Considering potential emergencies where individuals might gather in groups to improve their chances of survival, the experimental environment parameters were set as $A = \{16, 36, 64\}$ hectares, with $k = \{2, 8, 16, 50, 100\}$ targets grouped into $c = \{1, 5, 10\}$ clusters. Each group had a designated leader responsible for determining the group's trajectory. The target configurations included scenarios with both limited and substantial numbers of targets and scenarios characterized by low or high target concentration.

In light of the need to search for targets in the shortest possible time — an essential factor in SAR missions — we set specific initial mission parameters. These parameters included $n = \{2, 4, 8, 16, 32, 64\}$ UAVs, $T = \{900, 1200, 1800\}$ seconds, $t_s = 1$ second, $r_c = 20$ meters, $h = 20$ meters, and the initial waypoints $W_i$ were generated based on $A$, $n$, and the chosen CPP scan method. The UAVs operated at 10 m/s, while the targets moved at up to 5 m/s.

## VI. Results

Before conducting an exhaustive simulation of various scenarios, we performed a preliminary analysis of eight CPP approaches by running each possible scenario five times to identify which methods could effectively generate the initial waypoints $W_i$ (initial path) for each $u_i$ involved in the mission. The goal of this analysis was to improve the mission's outcomes. In this experiment, the LMAT method yielded the best results, demonstrating a median accuracy rate generally higher than that of the other CPP scanning methods.

After selecting LMAT as the CPP scan method to generate the UAV's initial paths ($W_i$), a set of 648 scenarios was created from all possible combinations of the initial parameters outlined in Section V and executed 15 times. The comprehensive analysis assessed how different scenarios influenced both the accuracy rate and, ultimately, the success rate of mission execution. It took into account the number of UAVs involved in the missions, the number of targets being pursued, and their distribution across the search area, which was defined by the concentration rate ($C$) (see eq. 6). This rate is measured in terms of targets per hectare.

Figure 3 illustrates the variation in the accuracy rate (ranging from 0% to 100%) along the y-axis for various scenarios involving 2, 4, 8, 16, 32, and 64 UAVs. The target concentration along the x-axis varies from 0.1 targets per hectare to 5 targets per hectare. Elevated values on the y-axis indicate a higher number of targets identified during the mission, achieving mission completion when the accuracy rate reaches 100%. Conversely, lower concentrations on the x-axis represent a more dispersed distribution of targets, which increases the amount of non-interest areas. In contrast, a higher concentration results in an expansion of areas of interest.

The results shown in Figure 3 reveal that accuracy improves significantly as the number of UAVs increases. Analyzing the median point of the box plot, we observe that this growth in accuracy follows a quadratic pattern. The fitted curve indicates that accuracy initially increases rapidly with the addition of UAVs but begins to plateau around $n = 16$. This suggests that while a higher UAV density enhances search efficiency, larger UAV swarms yield marginal gains.

Considering the impact of the concentration rate, it can be observed that for higher concentration rates ($C \geq 0.26$), the accuracy rate for $n \geq 16$ remains relatively constant at approximately 90%. For $n < 16$, accuracy appears more unstable, particularly for $n = 2$, as this number of UAVs is insufficient to cover an adequate search area within an average battery duration of UAVs considered to define $T$. The data also suggests that the concentration rate affects the algorithm's performance less than the number of UAVs involved in the mission.

The impact of clustering on the accuracy rate is illustrated in Figure 4. In this figure, the y-axis represents the accuracy rate, and the x-axis represents the number of target clusters. A

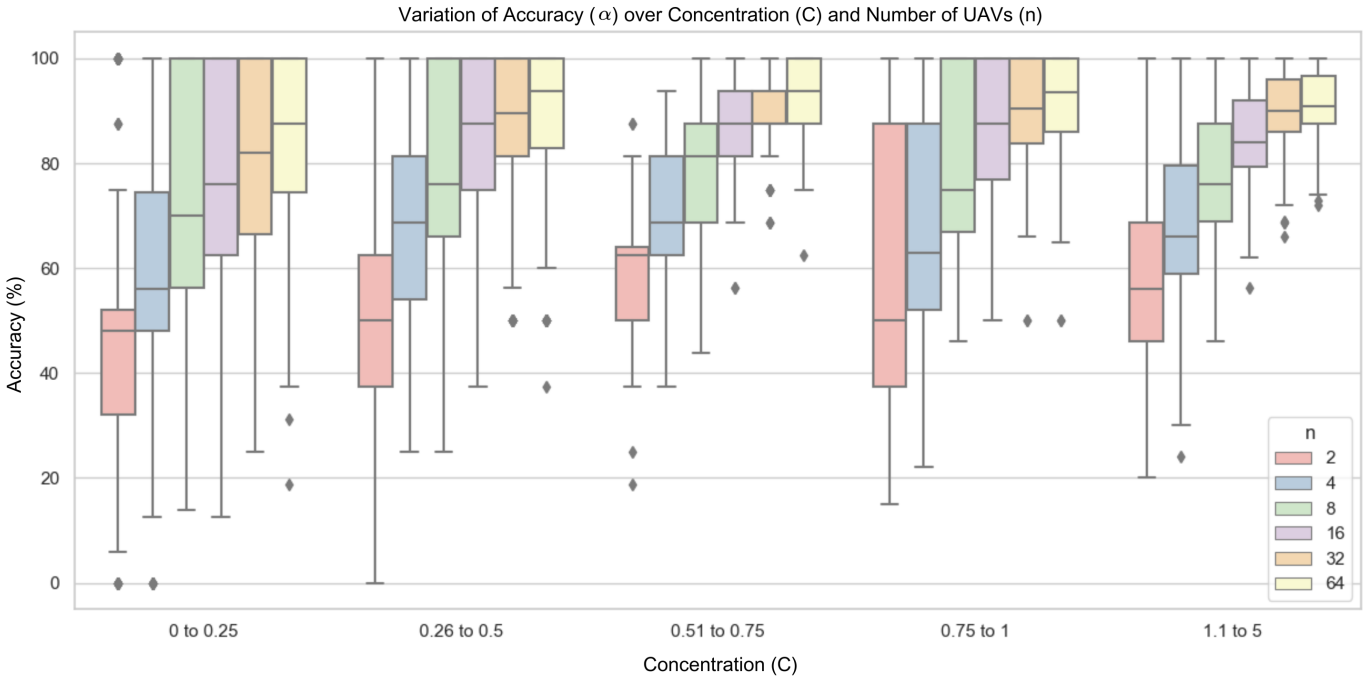


Figure 3. Accuracy of mission target detection ($\alpha$) versus concentration rate. (eq. 6)

higher value on the x-axis indicates that targets are distributed across more clusters, resulting in a higher target dispersion within the search area. In contrast, a value of one cluster means that all targets are concentrated in a single search area.

The figure shows a direct proportional relationship between clustering and density: as the number of clusters increases, the accuracy rate rises, while the area decreases. However, as the dispersion increases, the results for $n \geq 16$ become increasingly similar, indicating that improving the clustering significantly affects the accuracy results of the proposed approach more than simply increasing the number of UAVs to $n > 16$. It also suggests that environments with higher concentrations ($C > 1$) exhibit more stability and accuracy across all UAV densities, suggesting that clustered targets are easier to detect. The results support the expected outcomes of the proposal approach, which was designed for applications where targets tend to move together following a specific movement pattern.

## VII. Conclusions and Future Work

This study defines and implements an approach using multi-UAV collaboration and information fusion to dynamically identify areas with the highest probability of containing one or more mobile targets in unknown areas under time con-

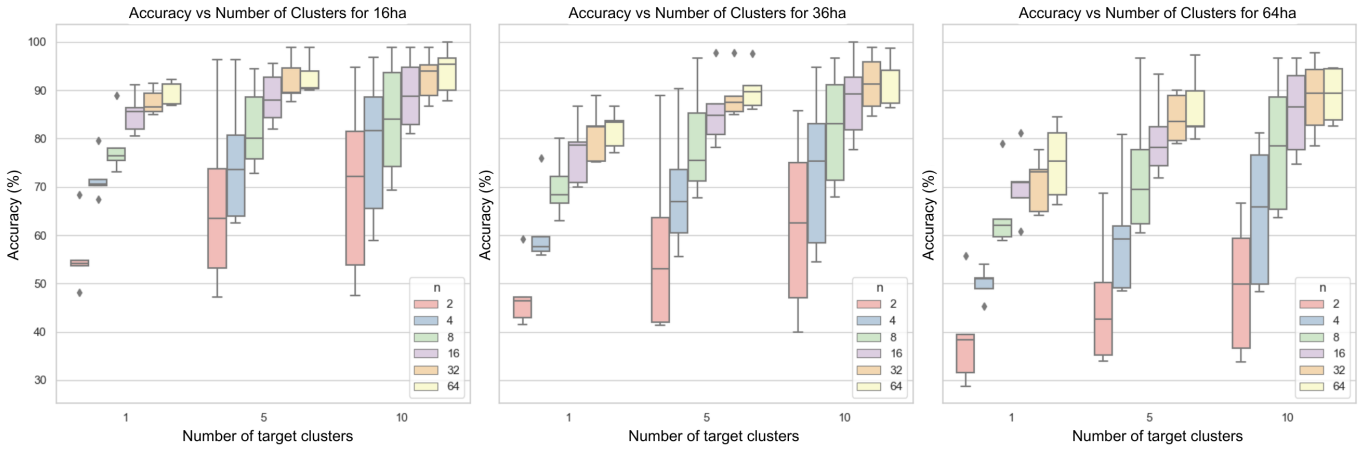


Figure 4. Accuracy of mission target detection ($\alpha$) versus Number of target clusters per area ($A$)

straints. The implementation is carried out using the Gradys-SIM-nextgen simulator. The continuous exchange of spatial awareness data between the UAVs includes the areas covered and those yet to be covered by each drone. The exchange among UAVs within the same group enhances the collective decision-making process for replanning routes. It ensures broader coverage to identify the maximum number of targets within the mission time.

A series of scenarios were created, varying the parameters of the search area ($A$), the number of UAVs ($n$), the number of targets ($k$), and the mission duration ($T$). The simulations performed for these scenarios produced the results presented in Section VI. These results indicate that the algorithm is highly effective in scenarios where $n \geq 16$ and $C > 0.25$. Specifically, accuracy reaches a plateau when $n = 16$, maintaining an average accuracy rate of 90%. These results suggest that in environments with a higher target concentration, an optimal team size of UAVs exists beyond which operational efficiency stabilizes.

Based on our findings and experiences implementing the solution, we expect to improve or maintain high detection rates with fewer drones or reduced tracking time by enhancing the coordination algorithm and incorporating support for scenarios where targets exhibit unpredictable movement patterns.

## REFERENCES


[1] Y. Alqudsi and M. Makaraci, "UAV swarms: research, challenges, and future directions," *Journal of Engineering and Applied Science*, vol. 72, pp. 12–35, 1 2025.

[2] S. Javed, A. Hassan, R. Ahmad, W. Ahmed, R. Ahmed, A. Saadat, and M. Guizani, "State-of-the-Art and Future Research Challenges in UAV Swarms," *IEEE Internet of Things Journal*, 2024.

[3] M. Cavalcanti, B. Olivieri, T. Lamenza, and M. Endler, "Pasture-based Livestock Identification and Counting by Coordenated UAVs," in *XLII Simposio Brasileiro de Redes de Computadores e Sistemas Distribuidos (SBRC2024)*, May 2024.

[4] J. Cao, W. L. Leong, and R. S. Huat Teo, "A Highly Scalable, Robust and Decentralized Approach for Multi-UAV Persistent Surveillance," in *2024 International Conference on Unmanned Aircraft Systems (ICUAS)*, pp. 971–977, June 2024.

[5] A. McConville, G. Tzoumas, L. R. Salinas, M. Munera, and S. Hauert, "Adoption of UAV Swarm Technology: Survey and Opinions of Firefighters," in *2024 IEEE International Conference on Advanced Robotics and Its Social Impacts (ARSO)*, pp. 228–234, May 2024.

[6] M. Bakirci and M. M. Ozer, "Post-Disaster Area Monitoring with Swarm UAV Systems for Effective Search and Rescue," in *2023 10th International Conference on Recent Advances in Air and Space Technologies (RAST)*, pp. 1–6, June 2023.

[7] M. Lyu, Y. Zhao, C. Huang, and H. Huang, "Unmanned Aerial Vehicles for Search and Rescue: A Survey," *Remote Sensing*, vol. 15, no. 13, 2023.

[8] E. Yanmaz, H. M. Balanji, and I. Guven, "Dynamic Multi-UAV Path Planning for Multi-Target Search and Connectivity," *IEEE Transactions on Vehicular Technology*, 2024.

[9] E. T. Alotaibi, S. S. Alqefari, and A. Koubaa, "LSAR: Multi-UAV Collaboration for Search and Rescue Missions," *IEEE Access*, vol. 7, pp. 55817–55832, 2019.

[10] S. A. H. Mohsan, N. Q. H. Othman, Y. Li, M. H. Alsharif, and M. A. Khan, "Unmanned aerial vehicles (UAVs): practical aspects, applications, open challenges, security issues, and future trends," *Intelligent Service Robotics*, vol. 16, pp. 109–137, 3 2023.

[11] B. J. Olivieri de Souza and M. Endler, "Ventures, Insights, and Ponderings from Real-World Experiments with FANETs and UAVs," *29th IEEE Symposium on Computers and Communications (IEEE ISCC 2024)*, pp. 1–7, 6 2024.

[12] Y. Luo, Z. Zhuang, N. Pan, C. Feng, S. Shen, F. Gao, H. Cheng, and B. Zhou, "Star-Searcher: A Complete and Efficient Aerial System for Autonomous Target Search in Complex Unknown Environments," *IEEE Robotics and Automation Letters*, vol. 9, pp. 4329–4336, May 2024.

[13] X. Cao, M. Li, Y. Tao, and P. Lu, "HMA-SAR: Multi-Agent Search and Rescue for Unknown Located Dynamic Targets in Completely Unknown Environments," *IEEE Robotics and Automation Letters*, vol. 9, pp. 5567–5574, June 2024.

[14] C. de Koning and A. Jamshidnejad, "Hierarchical integration of model predictive and fuzzy logic control for combined coverage and target-oriented search-and-rescue via robots with imperfect sensors," *Journal of Intelligent & Robotic Systems*, vol. 107, no. 3, p. 40, 2023.

[15] N. A. Kyriakakis, M. Marinaki, N. Matsatsinis, and Y. Marinakis, "A cumulative unmanned aerial vehicle routing problem approach for humanitarian coverage path planning," *European Journal of Operational Research*, vol. 300, pp. 992–1004, 8 2022.

[16] Z. Qadir, M. H. Zafar, S. K. R. Moosavi, K. N. Le, and M. A. Mahmud, "Autonomous UAV Path-Planning Optimization Using Metaheuristic Approach for Predisaster Assessment," *IEEE Internet of Things Journal*, vol. 9, pp. 12505–12514, 7 2022.

[17] J. Wu, Y. Sun, D. Li, J. Shi, X. Li, L. Gao, L. Yu, G. Han, and J. Wu, "An Adaptive Conversion Speed Q-Learning Algorithm for Search and Rescue UAV Path Planning in Unknown Environments," *IEEE Transactions on Vehicular Technology*, vol. 72, pp. 15391–15404, 12 2023.

[18] H. Gupta and O. P. Verma, "A novel hybrid Coyote–Particle Swarm Optimization Algorithm for three-dimensional constrained trajectory planning of Unmanned Aerial Vehicle," *Applied Soft Computing*, vol. 147, p. 110776, 2023.

[19] M. A. Alanezi, H. R. Bouchekara, T. A. A. Apalara, M. S. Shahriar, Y. A. Sha'aban, M. S. Javaid, and M. A. Khodja, "Dynamic Target Search Using Multi-UAVs Based on Motion-Encoded Genetic Algorithm With Multiple Parents," *IEEE Access*, vol. 10, pp. 77922–77939, 2022.

[20] Y. Wu and K. H. Low, "Route Coordination of UAV Fleet to Track a Ground Moving Target in Search and Lock (SAL) Task Over Urban Airspace," *IEEE Internet of Things Journal*, vol. 9, pp. 20604–20619, 10 2022.

[21] J. Houssineau, C. Xue, H. Cai, M. Uney, and E. Delande, "Decentralised multi-sensor target tracking with limited field of view via possibility theory," in *2024 27th International Conference on Information Fusion (FUSION)*, pp. 1–8, July 2024.

[22] K. Arulkumaran, M. P. Deisenroth, M. Brundage, and A. A. Bharath, "Deep reinforcement learning: A brief survey," *IEEE Signal Processing Magazine*, vol. 34, no. 6, pp. 26–38, 2017.

[23] L. Chang, L. Shan, C. Jiang, and Y. Dai, "Reinforcement based mobile robot path planning with improved dynamic window approach in unknown environment," *Autonomous robots*, vol. 45, pp. 51–76, 2021.

[24] D. Zorbas, L. Di Puglia Pugliese, T. Razafindralambo, and F. Guerriero, "Optimal drone placement and cost-efficient target coverage," *Journal of Network and Computer Applications*, vol. 75, pp. 16–31, 2016.

[25] R. Dai, S. Fotedar, M. Radmanesh, and M. Kumar, "Quality-aware UAV coverage and path planning in geometrically complex environments," *Ad Hoc Networks*, vol. 73, pp. 95–105, 2018.

[26] L. Lamport, "Fast Paxos," *Distrib. Comput.*, vol. 19, p. 79–103, Oct. 2006.

[27] B. Cornwell and J.-M. Ho, "Network Structure in Small Groups and Survival in Disasters," *Social Forces*, vol. 100, pp. 1357–1384, 04 2021.

[28] T. Lamenza, J. Kamysek, B. Souza, and M. Endler, " Developing Algorithms for the Internet of Flying Things Through Environments With Varying Degrees of Realism," in *Anais Estendidos do XLII Simpósio Brasileiro de Redes de Computadores e Sistemas Distribuídos*, (Porto Alegre, RS, Brasil), pp. 33–40, SBC, 2024.

[29] T. Lamenza, M. Paulon, B. Perricone, B. Olivieri, and M. Endler, "GrADyS-SIM - A OMNET++/INET simulation framework for Internet of Flying things," in *Anais Estendidos do XL Simpósio Brasileiro de Redes de Computadores e Sistemas Distribuídos*, (Porto Alegre, RS, Brasil), pp. 9–16, SBC, 2022.

[30] T. Lamenza, J. Kamysek, B. Souza, and M. Endler, "GrADyS-SIM simulator.." Available at: https://github.com/Project-GrADyS/gradys-simulations, 2021.

[31] OMNet++, "OMNeT++ : Discrete Event Simulator." Available at:https://omnetpp.org/, 2022.